CHEMICAL ENGINEERING TRANSACTIONS

VOL. 103, 2023

A publication of AIDIC
The Italian Association of Chemical Engineering
Online at www.cetjournal.it

Guest Editors: Petar S. Varbanov, Panos Seferlis, Yee Van Fan, Athanasios Papadopoulos

ISBN 979-12-81206-02-1; **ISSN** 2283-9216

DOI: 10.3303/CET23103019

Model Predictive Control on Integrated-Rooftop Greenhouse Climate Control

Wei-Han Chen*, Fengqi You

Cornell University, Ithaca, New York, 14853, USA
wc593@cornell.edu

A novel model predictive control (MPC) framework is proposed to optimize the energy management of integrated rooftop greenhouses and buildings, aiming to reduce control costs and the likelihood of climate violations. The centralized intelligent control approach employed for both the integrated rooftop greenhouse and the building ensures optimal conditions for crops and occupants. The integrated rooftop greenhouse utilizes waste heat and air from the building, resulting in reduced energy and CO_2 consumption. The nonlinear dynamic models of temperature, humidity, and CO_2 concentration for integrated rooftop greenhouse climate and building are first constructed. An integrated optimization problem is then formulated to acquire the optimal control decisions. The proposed MPC framework is implemented to regulate temperature, humidity, and CO_2 level via controlling fans, pad cooling, shades, heating, ventilation and air conditioning systems, CO_2 injection, and lighting systems. The indoor climate of an integrated rooftop greenhouse on a building in Brooklyn, New York, is controlled for the case study to show the advantages of the proposed nonlinear model predictive control framework. The results show that the average energy savings from the building to the integrated rooftop greenhouse amount to 15.2 % with the integration of the i-RTG and the host building under the proposed MPC framework.

1. Introduction

The rapid increase in urban populations, estimated to reach an additional 2.5 billion through population growth and urbanization by 2050 (Specht et al. 2014), necessitates addressing the issue of meeting the nutritional needs of the increasing population. The transportation and distribution of food into urban areas contribute to increased fossil fuel consumption, greenhouse gas emissions, and traffic congestion (Orsini et al., 2013). Consequently, interest in building-integrated agriculture (BIA) in urban regions has emerged (Montero et al., 2017). BIA is a food production approach utilizing the space and resources of a building (Appolloni et al., 2021). One popular application is rooftop greenhouses (RTGs), which are greenhouses built on the rooftop of buildings using the vacant area in urban. However, safely and efficiently controlling the indoor climate of an integrated RTG (i-RTG) remains a challenge due to the increased complexity of energy optimization resulting from weather disturbances and building integration.

The indoor climate of an i-RTG requires a smart advanced control method to ensure an optimal environment for crops. Montero et al. (2017) assessed RTGs in regions with mild winters, evaluating potential improvements in productivity. The climate model of the RTG was discussed in this work. However, the study focused on conducting simulations on the energy models instead of advanced control strategies. Benis et al. (2017) introduced an environmental analysis workflow for BIA with models considering energy, water, and solar radiation. Three urban farming cases for tomato cultivation adopted the workflow to obtain useful insights for preliminary evaluations (Liang et al., 2018). However, there is no control aspect considered in this work. To date, there remains a gap in the development of advanced control frameworks for i-RTGs.

A novel nonlinear model predictive control (NMPC) framework for i-RTG and building climate control is proposed to reduce the combined CO_2 and energy costs. Dynamic models for the i-RTG and building climate, encompassing temperature, humidity, and CO_2 concentration, are initially developed. The dynamic models of temperature, humidity, and CO_2 level for the i-RTG and the host building are derived from the energy and mass balance models that include transpiration and photosynthesis rate approximations. Past weather data is

Paper Received: 01 April 2023; Revised: 30 April 2023; Accepted: 13 June 2023
Please cite this article as: Chen W.-H., You F., 2023, Model Predictive Control on Integrated-Rooftop Greenhouse Climate Control, Chemical Engineering Transactions, 103, 109-114 DOI:10.3303/CET23103019

collected to help develop the nonlinear climate model for the i-RTG and building. Subsequently, the proposed NMPC framework incorporates the nonlinear dynamic models for temperature, humidity, and CO_2 level. The NMPC framework determines the control decisions that minimize the total control costs by solving a nonlinear programming problem repetitively. The proposed NMPC framework is implemented in a receding horizon procedure to regulate temperature, humidity, and CO_2 concentration through fans, heating, ventilation, air conditioning (HVAC), pad cooling, blinds, CO_2 injection, and lighting system. Lastly, we conduct simulations for an i-RTG atop a building in Brooklyn, New York, to showcase the performance of the proposed NMPC.

2. Dynamic models of building-integrated rooftop greenhouse formulation

The i-RTG, as shown in Figure 1, is situated on top of a building, with energy, moisture, and CO_2 interconnected with the host building below. CO_2 and waste heat from the building can be utilized in the RTG. During the daytime, the building supplies cooler air to help cool the RTG, while waste heat from the building is directed to the RTG at night to maintain an optimal crop environment. The actuators considered in the model include fans, HVAC, blinds, humidifiers, lighting, and CO_2 injection. The optimal control decisions are obtained by the NMPC.

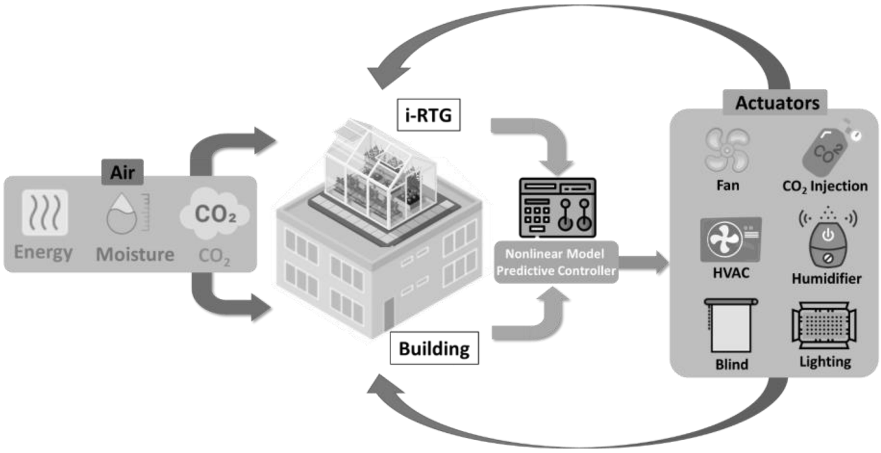

Figure 1: Overview of exchange flows of energy, moisture, and CO_2 between the i-RTG and the building. The control inputs of actuators are obtained by the NMPC controller. The system states, including temperature, humidity, and CO_2, are monitored

The system states of the RTG considered in this study include temperature, humidity, and CO_2 concentration (Hu and You, 2022). The relationships between system states, control inputs, and disturbances are captured by a nonlinear dynamic model (Chen et al., 2022). The developed model predicts the future state of the RTG climate, which is an essential component in the NMPC framework. The estimated future system state helps minimize control costs and prevent detrimental greenhouse climates for crop growth. Plant growth can be hindered by excessively low or high indoor temperatures. In addition, crop yield could be boosted by higher CO_2 levels during photosynthesis (Shamshiri et al., 2018a). On the other hand, elevated humidity may lead to mold growth, negatively impacting crop quality and yield (Mortensen, 1987). Consequently, these system states require specific constraints to safeguard plants (Chen and You, 2021). The primary factors influencing i-RTG temperature are solar radiation q_s, heat flux through the cover q_c, pad cooling q_{pd}, waste heat from supplemental lighting q_l, ventilation q_v, heating pipe q_p, and exhaust air from the building. The continuous-time i-RTG temperature dynamic model is shown (Lin et al., 2021):

$$\rho V C_a \frac{dT_i}{dt} = q_s + q_p + q_l - q_c - q_v - q_{pd} \tag{1}$$

where C_a, V, and ρ represent the air-specific heat, greenhouse volume, and air density.

$$q_s = A_s I_o K_a \left(1 - \tau_s u_{blind}\right) \tag{2}$$

$$q_p = \rho_w C_w K_h T_h u_{pipe,\max} u_{pipe} \tag{3}$$

$$q_l = \tau_l u_{light,\max} u_{light} \tag{4}$$

$$q_c = A_s K_c \left(T_i - T_o\right) \tag{5}$$

$$q_v = \rho C_a u_{fan,\max} \left(T_i - T_o\right) u_{fan} \tag{6}$$

$$q_{pd} = A_p K_p u_{pad,\max} \left(T_p - T_i\right) u_{pad} \tag{7}$$

where A_s, τ_s, K_a, and I_o denote the greenhouse surface area, shading percentage, coefficient of the solar equation, and outdoor global radiation. The control inputs of fan speed, heating pipe water flow rate, shade curtain, and pad shutter are represented by u_{pipe}, u_{fan}, u_{blind}, and u_{pad}. C_w and ρ_w represent the water-specific heat and water density. K_p, K_c, and K_h are the coefficients of the equations for pad cooling, cover equation, and heating pipe. T_p, T_o, and T_h denote the temperatures of air through the cooling pad, ambient temperature, and water in the heating pipe. A_p and τ_l are the pad area and heat conversion percentage.

To combine the dynamic humidity models for the RTG and the building, we first list the factors considered in the dynamic humidity models. The relative humidity is determined by temperature and absolute humidity. The absolute humidity is first considered in the mass balance equation (Ajagekar et al., 2023). The mass balance equation of absolute humidity in the RTG considers the water net flows from the fogging system m_{fog}, evapotranspiration of the plants m_{trans}, and the ventilation m_{vent}, and is given as:

$$\rho V \frac{\mathrm{d}h_i}{\mathrm{d}t} = m_{vent} + m_{trans} + m_{fog} \tag{8}$$

The photosynthetic rate is greatly affected by the CO_2 level and can be stimulated up to a certain rate when the CO_2 level is elevated. CO_2 concentration is an important factor in crop quality and yield. In the daytime, the CO_2 from occupants' respiration helps the fertilization of the i-RTG. The mass balance equation for CO_2 includes the CO_2 injection X_{inj}, net consumption by photosynthesis X_{pho}, and CO_2 net flow from ventilation X_{vent}, indoor CO_2 concentration level X_i, as shown below:

$$\rho V \frac{\mathrm{d}X_i}{\mathrm{d}t} = X_{vent} - X_{pho} + X_{inj} \tag{9}$$

The most important factor for thermal comfort is indoor temperature (Chen and You, 2022). A dynamic temperature model is needed for the NMPC to predict future temperatures (Hu et al., 2022). A popular approach to constructing a building dynamic temperature model is to take building components analogous to resistances and capacitances within an electric circuit (Yang et al., 2022). The resistance-capacitance model has shown effectiveness in past studies (Oldewurtel et al., 2013). The dynamic temperature model for a multi-zone building is generated through Building Resistance-Capacitance Modeling (BRCM) Toolbox in this work (Sturzenegger et al., 2016). The dynamic temperature model for a multi-zone building generated by BRCM is based on the building materials, structures, and geometry (Hu et al., 2023). The dynamics are shown as follows:

$$T_{k+1} = AT_k + B_u u_k + B_v v_k + \sum_{i=1}^{n_u} \left(B_{vu,i} v_k + B_{T_{u,i}} T_k\right) u_{k,i} \tag{10}$$

where T_k represents the temperatures of each room and building components, such as roof, floor, and walls. u_k denotes the control inputs, and v_k is the predicted disturbances (e.g., weather forecast). A, B_v, B_u, $B_{xu,i}$, and $B_{vu,i}$ are the system matrices.

Another important factor in building climate relating to thermal comfort is humidity (Zhang et al., 2014). The dynamic model for absolute humidity can first be developed using the mass balance equation on water (Xiao et al., 2023). The equation considering the water amount through ventilation, respiration, and control actuators is given as,

$$\rho V \frac{\mathrm{d}h_i}{\mathrm{d}t} = m_{vent} + m_{res} + m_{hum} \tag{11}$$

where h_i denotes absolute humidity, m_{vent} represents the ventilation, m_{res} is the occupant respiration, and m_{hum} denotes the net flow of control actuators for humidity.

The energy, moisture, and CO_2 are interconnected with the host building underneath. The CO_2 and waste heat from the building can be utilized in RTG. An NMPC framework is developed to control the i-RTG and building indoor climate. The objective of the optimization problem in the framework is to minimize the combined energy and CO_2 costs of the i-RTG and building.

NMPC is a suitable approach for i-RTG and building climate control. The nonlinear dynamic models presented in the previous section are derived into a compact form, where H denotes the prediction horizon. The compact form of the model includes the nonlinear vector function $\mathbf{f}(\cdot)$, control input $\mathbf{u}$, disturbance sequences $\mathbf{v}$, initial system states x_0, and system state $\mathbf{x}$, and can be written out as: $\mathbf{x} = \mathbf{f}(x_0, \mathbf{u}, \mathbf{v})$. Besides the nonlinear dynamic model, the constraints are also important components of the NMPC framework. The system states and control inputs constraints are defined by $\mathbf{G}_x \mathbf{x} \le \mathbf{g}_x$ and $\mathbf{G}_u \mathbf{u} \le \mathbf{g}_u$. $\mathbf{G}_x$, $\mathbf{g}_x$, $\mathbf{G}_u$, and $\mathbf{g}_u$ are the vectors defining the system states and control input constraints. The nonlinear optimization problem can be shown as:

$$
\begin{aligned}
\min_{u} \ & J = \mathbf{cc}^T \mathbf{u} + \boldsymbol{\varepsilon}^T \mathbf{S} \boldsymbol{\varepsilon} \\
\text{s.t.} \ & \mathbf{x} = \mathbf{f}(x_0, \mathbf{u}, \mathbf{v}) \\
& \mathbf{G}_x \mathbf{x} \le \mathbf{g}_x + \boldsymbol{\varepsilon} \\
& \mathbf{G}_u \mathbf{u} \le \mathbf{g}_u \\
& \boldsymbol{\varepsilon} \ge 0
\end{aligned}
\tag{12}
$$

where ε, S, and cc denote slack variables, constraint violation penalty weight matrix, and cost coefficients.
The proposed NMPC framework for i-RTG and building climate adopts a receding horizon approach. The weather forecast and system state data are first collected at each time step. The optimal control decisions can then be obtained by solving the nonlinear optimization problem. Among the sequence of optimal control inputs, only the control inputs for the first time step will be applied. The same procedure is followed in the next time step. The i-RTG and building climate are controlled by the NMPC framework when the control inputs are fed to actuators, including fans, HVAC, blinds, humidifiers, lighting, and CO_2 injection.

3. Case study on an integrated rooftop greenhouse and building

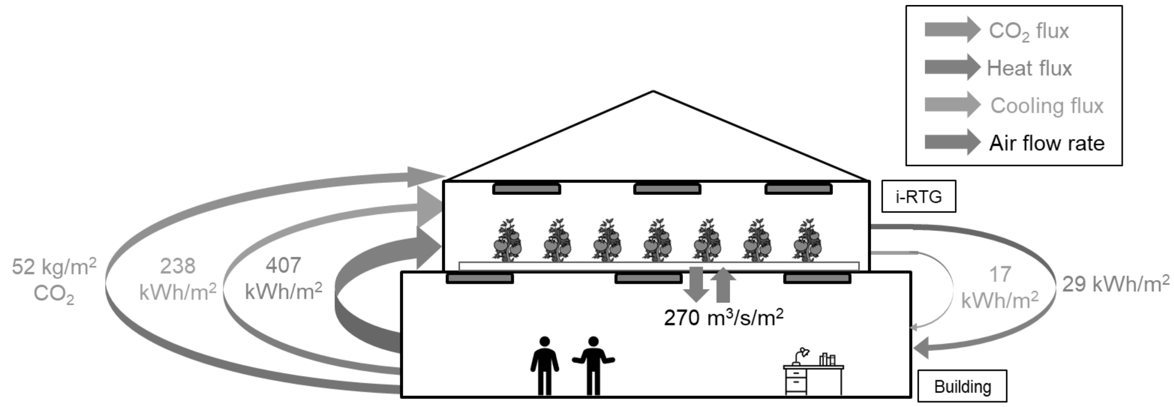

Figure 2: Interconnection flow between i-RTG and the building. The arrows on the left are the fluxes transferred from the host building to the i-RTG; the right-hand side arrows are the fluxes from the i-RTG to the host building

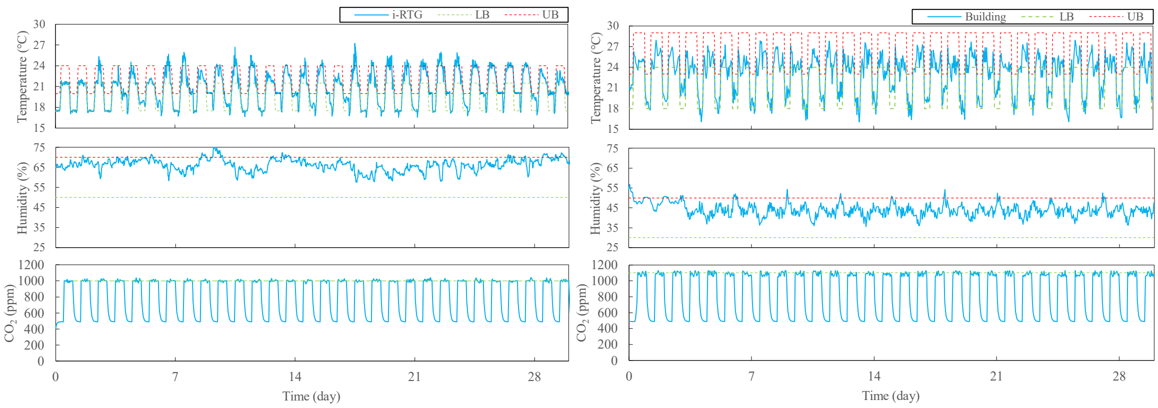

Figure 3: Control profiles of indoor climate in the (left) i-RTG and (right) host building for 30 days in winter during January 1-30, 2021. The lower and upper bounds are presented in red and green dotted lines

In this study, we consider an i-RTG in Brooklyn, New York, as the target greenhouse and building. The i-RTG dimension is 40 m × 13 m × 4 m. We simulate an i-RTG growing tomatoes for closed-loop indoor greenhouse climate control using the NMPC framework. Temperature, CO_2 level, and relative humidity inside the i-RTG and building are controlled in this work. Outdoor temperature, outdoor humidity, outdoor CO_2 level, and solar radiation are considered disturbances (Chen et al., 2022). Simulations are conducted for 60-day periods across four different seasons, commencing on January 1, April 1, July 1, and October 1 in 2021. Weather forecasts are gathered to solve the optimal control problem. The system state for the next time step is determined by the weather measurement data and the prediction model (Chen et al., 2022). The sampling interval of the NMPC controller is set as 15 min. The control horizon is set as 6 h. Figure 2 illustrates the interconnection flows between the i-RTG and the building, with CO_2 flux, heat flux, cooling flux, and air flow rate represented by green, red, blue, and grey arrows. The CO_2 flux is unidirectional, flowing only from the i-RTG to the building. The higher CO_2 concentration in the building, resulting from occupants' respiration during working hours, acts as a natural CO_2 fertilizer for the i-RTG, saving 52 kg/m^2 of CO_2 through integration with the building. Both heat flux and cooling flux are bidirectional, as the i-RTG and the building can help heat or cool each other depending on the time period. The heat flux from the building to the i-RTG and vice versa are 407 kWh/m^2 and 29 kWh/m^2, while the cooling flux values are 238 kWh/m^2 and 17 kWh/m^2. Due to the building's larger heat capacity, most energy is saved when air is transferred from the building to the i-RTG.

Figure 3 illustrates the control trajectories for indoor temperature, humidity, and CO_2 levels in the i-RTG and the building during January 1-30, 2021, winter season. The constraints for the i-RTG temperature are chosen distinctively over the day, accounting for the dark and light periods. The light and dark periods last from 4 am to 12 am and from 12 am to 4 am. As the i-RTG transitions between the light and dark periods, the lower and upper constraints are adjusted gradually to circumvent sudden alterations in greenhouse temperature. A discernible diurnal pattern is evident, and the system state is kept in the region demarcated by the lower and upper constraints. Constraint violations occasionally arise because of forecast errors. For the i-RTG, humidity lower and upper constraints are suggested to be 50 % and 70 % (Shamshiri et al., 2018b). During winter, the humidity profile is better maintained within these constraints than those temperature trajectories. As the outdoor air has less humidity than the indoor air on colder days, the ventilation system assists in drawing ambient air when humidity exceeds the upper bound. CO_2 injections occur from 4 am to 12 am during the light period, maintaining CO_2 levels around 1,000 ppm to boost crop growth. CO_2 injections cease in the dark period, allowing the CO_2 level to gradually drop to ambient levels due to ventilation.

Table 1: Energy consumption from the fan, HVAC, pad cooling system, CO_2 injection, and lighting systems of the sum of i-RTG and building compared with stand-alone building and greenhouse

	Stand-alone building (kWh/m^2)	Stand-alone greenhouse (kWh/m^2)	i-RTG + building (kWh/m^2)	Savings percentage comparing stand-alone with integration
Winter	174	127	278	7.6 %
Spring	129	99	170	25.4 %
Summer	161	71	212	8.6 %
Fall	121	81	163	19.3 %
Average	593	378	823	15.2 %

Table 1 compares energy consumption in the i-RTG and the building across all seasons. Stand-alone building and stand-alone greenhouse cases are evaluated, where no integration exists between the two, and contrasted with the integrated case. Energy savings primarily occur at nighttime, especially during winter, with a 7.6 % reduction when the i-RTG and building are integrated. Energy is conserved by transferring the air from the building to the greenhouse when i-RTG temperatures drop at night. A substantial 25.4 % saving is achieved in spring due to New York's cool weather, while summer savings are less significant, resulting in an average energy saving of 15.2 % from building to i-RTG.

4. Conclusions

In this study, we proposed an NMPC framework to regulate temperature, humidity, and CO_2 levels in an i-RTG and building indoor climate. Energy and mass balance equations were employed to generate nonlinear dynamic models for the i-RTG and building climate, encompassing temperature, humidity, and CO_2 level. A nonlinear optimization problem that incorporates the dynamic models was then formulated for the purpose of determining the optimal control decisions for the i-RTG and building indoor climate. The proposed NMPC framework with the receding horizon approach generated the optimal control trajectory. The stability and feasibility issues of the proposed framework for controlling i-RTG and building climate were assessed. A case study was conducted for a 60-day production period across different seasons, focusing on the regulation of indoor temperature, relative humidity, and CO_2 concentration levels in an i-RTG and building located in Brooklyn, New York. The results demonstrated that the proposed NMPC framework could effectively minimize the total control costs for both the i-RTG and the building.

References

Ajagekar A., Mattson N.S., You F., 2023, Energy-efficient AI-based Control of Semi-closed Greenhouses Leveraging Robust Optimization in Deep Reinforcement Learning. Advances in Applied Energy, 9, 100119.

Appolloni E., Orsini F., Specht K., Thomaier S., Sanyé-Mengual E., Pennisi G., Gianquinto G., 2021, The global rise of urban rooftop agriculture: A review of worldwide cases. Journal of Cleaner Production, 296, 126556.

Benis K., Reinhart C., Ferrão P., 2017, Development of a simulation-based decision support workflow for the implementation of building-integrated agriculture in urban contexts. Journal of Cleaner Production, 147, 589.

Chen W.-H., Mattson N.S., You F., 2022, Intelligent control and energy optimization in controlled environment agriculture via nonlinear model predictive control of semi-closed greenhouse. Applied Energy, 320, 119334.

Chen W.-H., You F., 2021, Smart greenhouse control under harsh climate conditions based on data-driven robust model predictive control with principal component analysis and kernel density estimation. Journal of Process Control, 107, 103-113.

Chen W.-H., You F., 2022, Sustainable building climate control with renewable energy sources using nonlinear model predictive control. Renewable and Sustainable Energy Reviews, 168, 112830.

Hu G., You F., 2022, Renewable energy-powered semi-closed greenhouse for sustainable crop production using model predictive control and machine learning for energy management. Renewable and Sustainable Energy Reviews, 168, 112790.

Hu G., You F., 2023, Multi-zone building control with thermal comfort constraints under disjunctive uncertainty using data-driven robust model predictive control. Advances in Applied Energy, 9, 100124.

Liang Y., Hui C.W., You F., 2018, Multi-objective economic-resource-production optimization of sustainable organic mixed farming systems with nutrient recycling. Journal of Cleaner Production, 196, 304-330.

Lin D., Zhang L., Xia X., 2021, Model predictive control of a Venlo-type greenhouse system considering electrical energy, water and carbon dioxide consumption. Applied Energy, 298, 117163.

Montero J.I., Baeza E., Heuvelink E., Rieradevall J., Muñoz P., Ercilla M., Stanghellini C., 2017, Productivity of a building-integrated roof top greenhouse in a Mediterranean climate. Agricultural Systems, 158, 14-22.

Mortensen L.M., 1987, CO2 enrichment in greenhouses crop responses. Scientia Horticulturae, 33, 1-25.

Oldewurtel F., Sturzenegger D., Morari M., 2013, Importance of occupancy information for building climate control. Applied Energy, 101, 521-532.

Orsini F., Kahane R., Nono-Womdim R., Gianquinto G., 2013, Urban agriculture in the developing world: a review. Agronomy for Sustainable Development, 33(4), 695-720.

Shamshiri R.R., Jones J.W., Thorp K.R., Ahmad D., Man H.C., Taheri S., 2018a, Review of optimum temperature, humidity, and vapour pressure deficit for microclimate evaluation and control in greenhouse cultivation of tomato: a review. International Agrophysics, 32, 287-302.

Shamshiri R.R., Kalantari F., Ting K.C., 2018b, Advances in greenhouse automation and controlled environment agriculture: a transition to plant factories and urban agriculture. Journal of Agricultural Engineering, 11, 22.

Specht K., Siebert R., Hartmann I., Freisinger U.B., Sawicka M., Werner A., Thomaier S., Henckel D., Walk H., Dierich A., 2014, Urban agriculture of the future: an overview of sustainability aspects of food production in and on buildings. Agriculture and Human Values, 31(1), 33-51.

Sturzenegger D., Gyalistras D., Morari M., Smith R.S., 2016, Model predictive climate control of a Swiss office building: Implementation, results, and cost–benefit analysis. IEEE Transactions on Control Systems Technology, 24, 1-12.

Xiao T., You F., 2023, Building thermal modeling and model predictive control with physically consistent deep learning for decarbonization and energy optimization. Applied Energy, 342, 121165.

Yang S., Gao H.O., You F., 2022, Model predictive control for Demand- and Market-Responsive building energy management by leveraging active latent heat storage. Applied Energy, 327, 120054.

Zhang T., Liu X., Jiang Y., 2014, Development of temperature and humidity independent control (THIC) air-conditioning systems in China—A review. Renewable and Sustainable Energy Reviews, 29, 793-803.